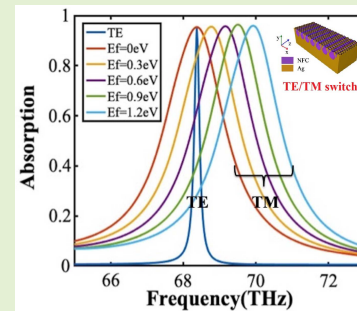


High-Performance Sensitive TE/TM Mode Switch With Graphene-Based Metal-Dielectric Resonances

Tairong Bai, Yang Tang, Zheng-Da Hu¹, Tonglu Xing, Zhiyu Lu, Yulan Huang, and Jicheng Wang¹

Abstract—We explore the performance of the monolayer graphene with a metal-dielectric compound grating via numerical simulation. The results show that the absorption peaks can be near 100% at 68.36 THz for both TE and TM polarizations. Different spectral line shapes are displayed under different polarization states, we attribute the excellent absorption performance to the excitation of magnetic resonance (MR) and cavity mode resonance (CMR), and then an equivalent capacitance-inductance (LC) circuit model and the waveguide theory are used to explain it theoretically. We have also studied the influence of the polarization angle on the absorption performance, and found that as the polarization angle increases, the resonance wavelength remains unchanged but the FWHM of absorption spectrum increases gradually. Based on this feature, we apply it in mode switch which can easily switch its function as absorption or sensing by adjusting the polarization states of incident radiations.

Index Terms—Compound metallic grating, coupled mode theory, graphene-based mode switch.



I. INTRODUCTION

METAMATERIAL is an artificial electromagnetic material with a size in the sub-wavelength range. The material itself has absorption loss attributed to the imaginary part of its optical indexes, which is beneficial to electromagnetic absorption devices for perfect absorption purpose. Perfect absorbers based on the metamaterial structures have attracted more and more attention. It plays an extremely crucial role in many occasions, such as filters, solar energy harvestings,

sensors, thermal emitters, absorbers and so on [1]–[7]. In 2008, Landy *et al.* [8] first proposed a kind of metamaterial absorber structure, which utilized electric ring resonators (EERs) and cut wires to achieve perfect absorption in the microwave field by coupling to electric and magnetic fields. Since then, metamaterial absorbers of various structures were proposed. J. Hao *et al.* [9] proposed a kind of metal-insulator-metal (MIM) structure to achieve plasmon resonance absorption in the visible light band; Ye *et al.* [10] proposed the phosphorus-spacer-metallic grating hybrid system, which achieved perfect absorption in the far-infrared band by implementing the strong coupling between black phosphorus surface plasmons (BPSP) and magnetic plasmons (MP). However, most of these studies are based on surface plasmon polaritons (SPPs) or magnetic resonators (MRs) to achieve perfect absorption, only the TM-polarized electromagnetic waves were employed to explore ideal absorption effect, whereas TE-polarized electromagnetic waves were rarely mentioned. Zou *et al.* [11] proposed a grating structure composed of two pairs of thin graphene dielectric layers, which achieved an angle-insensitive light absorber independent on polarizations. Shuo Liu *et al.* [12] achieved a broadband metamaterial absorber in the terahertz band by using multiple metallic bars. Despite these studies, TE / TM polarizations cannot be distinguished well yet, thus limiting their applications.

Manuscript received July 26, 2020; revised August 22, 2020; accepted August 22, 2020. Date of publication September 8, 2020; date of current version January 6, 2021. This work was supported in part by the National Natural Science Foundation of China (NSFC) under Grant 11504139, Grant 11504140, and Grant 11811530052; in part by the China Postdoctoral Science Foundation Grant 2017M611693 and Grant 2018T110440; in part by the Intergovernmental Science and Technology Regular Meeting Exchange Project of Ministry of Science and Technology of China under Grant CB02-20; in part by the Open Fund of State Key Laboratory of Applied Optics under Grant SKLAO2020001A04; and in part by the Training Programs of Innovation and Entrepreneurship for Undergraduates of Jiangsu Province and China under Grant 201910295051Z and Grant 201910295067. The associate editor coordinating the review of this article and approving it for publication was Dr. Carlos Marques. (Corresponding author: Jicheng Wang.)

Tairong Bai, Yang Tang, Zheng-Da Hu, Tonglu Xing, Zhiyu Lu, and Yulan Huang are with the School of Science, Jiangnan University, Wuxi 214122, China (e-mail: 1125412626@qq.com; 1831844383@qq.com; huyuanda1112@jiangnan.edu.cn; 1009700698@qq.com; 1461512755@qq.com).

Jicheng Wang is with the School of Science, Jiangnan University, Wuxi 214122, China, and also with the State Key Laboratory of Applied Optics, Changchun Institute of Optics, Fine Mechanics and Physics, Chinese Academy of Sciences, Changchun 130033, China (e-mail: jcwang@jiangnan.edu.cn).

Digital Object Identifier 10.1109/JSEN.2020.3022682

1558-1748 © 2020 IEEE. Personal use is permitted, but republication/redistribution requires IEEE permission.

See <https://www.ieee.org/publications/rights/index.html> for more information.

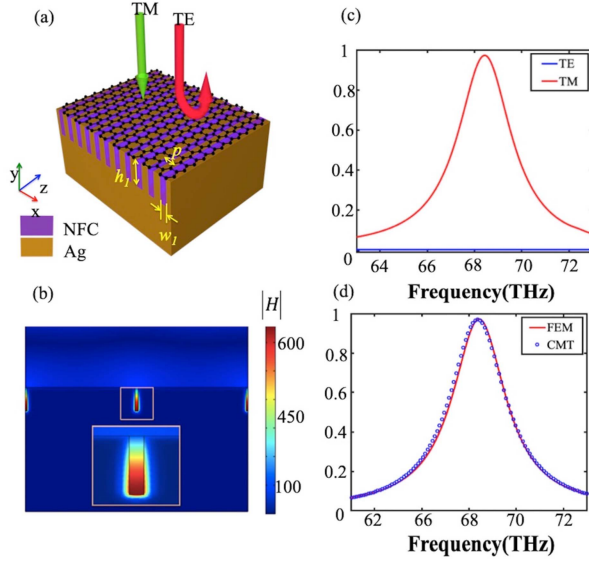


Fig. 1. (a) Schematic of the proposed one-dimensional absorber based on metal-dielectric resonance structure. (b) Magnetic field distribution ($|H|$) at resonant frequency for TM polarization. (c) FEM simulated absorption spectrum of proposed structure for TE and TM polarization. (d) FEM simulated and CMT fitted absorption spectrum for TM polarization. We set wavelength of $\lambda = 632.8$ nm under TM-polarized.

absorption peak. By contrast, when TE polarized electromagnetic wave irradiates this structure, it can excite cavity mode resonance (CMR) in the circular resonators, which restricts most of the electromagnetic field in the structure and form a narrow band absorption peak. We separately investigate the influences of the geometric parameters of these two cavities on the absorption performance and use the equivalent inductance-capacitance (LC) circuit model and coupled-mode theory (CMT) to explain them theoretically. Moreover, both of these resonators are insensitive to the angle of incidence. We can imagine that when the polarization angle of the incident wave changes from 0° to 90° (from TE polarization to TM polarization), the absorption spectrum undergoes a continue increase. Based on such phenomenon, we can use it to realize a TE / TM mode switch with many superior performances. Moreover, our design is a simple one-dimensional grating structure, whose working mechanism can be clearly studied.

II. THE ABSORPTION PERFORMANCE OF NARROW SLITS AND ITS THEORETICAL EXPLANATION

Fig. 1 (a) shows a one-dimensional metallic grating composed of a series of narrow slits, and this structure is covered by a monolayer graphene. The grating constant is $p = 2.3 \mu\text{m}$. The width and height of the narrow cavity are $w_1 = 49.4$ nm and $h_1 = 0.476 \mu\text{m}$ respectively. The substance filled in the cavity is a kind of dielectric with the permittivity of 2.4 such as NFC, which is a kind of organic polymer. The dielectric constant of silver can be described by the Drude model [13]

$$\varepsilon = \varepsilon_\infty - \frac{\omega_p}{\omega^2 + i\gamma\omega}, \quad (1)$$

with the plasma frequency $\omega_p = 1.39 \times 10^{16}$ rad/s, scattering rate $\gamma = 2.7 \times 10^{13}$ rad/s and high-frequency parameters $\varepsilon_\infty = 3.4$. For the monolayer graphene, its surface conductivity is associated with the incident angular frequency ω , Fermi

energy E_f and electron relaxation time τ (given by $\tau = \mu E_f$). It follows the expression [14], [15]:

$$\sigma_g = \frac{ie^2 E_f / \pi \hbar^2}{\omega + i\tau^{-1}} \quad (2)$$

in which e and \hbar are the electron charge and the reduced Plank constant respectively, and μ represents the direct current mobility of monolayer graphene. In our simulation the value of τ is set as $10 \text{ m}^2/(\text{V}\cdot\text{S})$, and then the permittivity of graphene layer is given by [16], [17]:

$$\varepsilon_g = \varepsilon_r + \frac{\sigma_g}{\omega \varepsilon_0 t_0}. \quad (3)$$

Here t_0 is the thickness of graphene which is set as 1nm.

Now we consider a radiation incident on the grating from the air at a normal incident angle. Due to the high reflectivity of the metal, the absorption of the narrow slits is often very low, but when the resonance occurs in the cavity, the reflectivity will suddenly decrease, thus forming an absorption peak. We use the finite element method (FEM) to calculate the absorption spectrum, and Fig. 1(b) shows the magnetic field distribution when resonance occurs in the slits, it can be found that most of the magnetic field are well localized in these narrow slits. Fig. 1(c) shows the absorption spectrum under TE and TM polarization. For TM polarization (electric field along the z-axis), the incident radiation can excite resonance at the frequency of 68.36 THz, thus generating an absorption peak with absorption rate exceeding 98%. However, it cannot excite any resonance mode under TE polarization (electric field along the x-axis). As for the absorption spectrum of this system, we can explain it theoretically by using coupled mode theory (CMT), which is used to describe the input, output and loss characteristics of a resonant cavity. Now we consider a system without transmission loss such as the structure shown in Fig. 1(a) with stored energy $|a|^2$ in a single resonance at ω_0 , and it will interact with input and output radiation with amplitude a^- and a^+ . Using the CMT formalism, the system can be described as [18], [19]

$$\frac{da}{dt} = (i\omega_0 - \gamma_e - \delta)a + \sqrt{2\gamma_e}a^+, \quad (4)$$

$$a^- = \sqrt{2\gamma_e}ea - a^+, \quad (5)$$

where γ_e is the intrinsic loss rate due to the material absorption, and δ is the external leakage rate due to the coupling of resonance to the outgoing wave. Then the reflection of the system can be written as

$$R = \frac{a^-}{a^+} = \frac{i(\omega - \omega_0) + \delta - \gamma_e}{i(\omega - \omega_0) + \delta + \gamma_e}, \quad (6)$$

therefore the expression of absorption is given by:

$$A = 1 - |R|^2 = \frac{4\delta\gamma_e}{(\omega - \omega_0)^2 - (\delta + \gamma_e)^2}. \quad (7)$$

It can be found from Fig. 1(d) that the results given by the CMT are basically consistent with those of FEM simulation results.

As for the TM polarization, the absorption peak is generated due to the strong coupling between magnetic resonance in the micro-nano structure and the external electromagnetic waves. When the radiation is incident on such a grating structure,

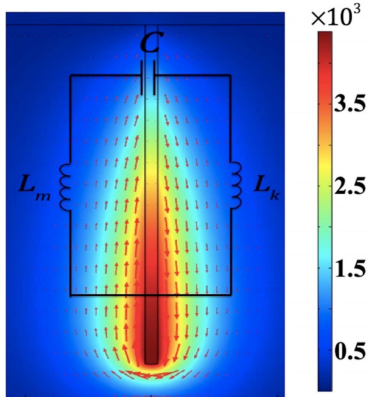


Fig. 2. The magnetic field and current-density distribution at resonant frequency, the circuit in the figure is the equivalent LC circuit of this system.

induced current can be generated inside the metal around the narrow slits. Then the oscillating induced current and the electric field in the dielectric can form a closed loop. Therefore, for this case, an equivalent LC circuit model [15] can be introduced to predict the magnetic resonance conditions. The dielectric filled in the narrow cavity can be equivalent to a capacitor, which can be expressed as:

$$C = c_1 \varepsilon_0 \varepsilon_d \frac{h_1 l}{w_1}, \quad (8)$$

where c_1 is a numerical factor ranging from 0 to 1 which is related to the distribution of charge on the metal conductor. In this system, it is taken as 0.467. ε_0 and ε_d are the electric permittivity of vacuum and dielectric respectively, and l is the length in the y direction. For a one-dimensional grating structure, it can be taken as the unit length.

Fig. 2 illustrates the electromagnetic field and current-density distribution at the resonant frequency, it is the structure that have formed a closed loop around the slits, and the current is contributed by two parts: displacement current and induced current. So we can use the equivalent LC circuit model [20], [21] to predict the resonance condition of this system. The metal conductor around the slits can be equivalent to an inductive element, which consists of kinetic inductance L_k and mutual inductance L_m , the expressions given by

$$L_k = -\frac{2h_1 + w_1}{\varepsilon_0 \omega^2 l \delta} \frac{\varepsilon'}{\varepsilon'^2 + \varepsilon''^2}, \quad (9)$$

$$L_m = \mu_0 \frac{h_1 w_1}{l}, \quad (10)$$

where ω is the angular frequency of the incident electromagnetic wave, ε' and ε'' are the real and imaginary parts of the electric permittivity ε respectively, and $\delta = \lambda/2\pi\kappa$ is the penetration depth with κ being the extinction coefficient, which can be calculated by the formula $\varepsilon = (n + i\kappa)^2$, and μ_0 is the permeability of vacuum. Therefore, the total impedance of the equivalent LC circuit can be expressed as:

$$Z = i\omega \left(L_k + L_m - \frac{1}{\omega^2 C} \right). \quad (11)$$

When the total impedance value is set as 0, then the expression of the magnetic resonance frequency can be obtained as:

$$f_R = \frac{1}{2\pi \sqrt{(L_k + L_m) C}}. \quad (12)$$

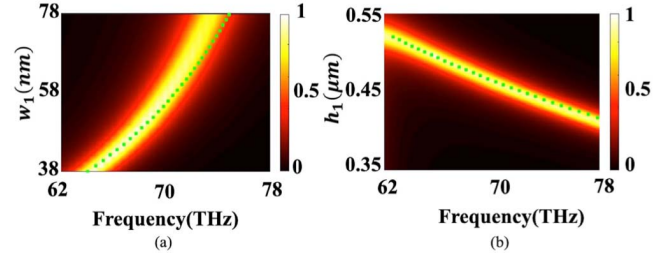


Fig. 3. The absorption spectrum as a function of frequency and width w_1 (a), depth h_1 (b) for TM polarization. The green square marks are the results from equivalent LC circuit model.

It is worth mentioning that l does not appear in the equation, indicating that the resonance frequencies of a 1D grating and a 2D grating with the same geometry parameters are the same. The theoretical value of the resonance frequency obtained according to the above formula is 68.4 THz, which is very close to the simulation results. The result shows that the equivalent LC circuit model can explain the absorption characteristics of the one-dimensional grating very well.

In Fig. 3 we have studied the influence of geometric parameters of these narrow slits on the absorption performances of this system. Obviously, with the increase of the cavity width w_1 , the magnetic resonance wavelength will show a significant blue-shift phenomenon, and its peak absorption rate is always maintained above 90%. As for the depth of slits h_1 , when its value is increased, the resonance frequency will undergo a significant redshift. Thus, we can change the working frequency of the system by adjusting the geometric parameters of the narrow slits. The curve marked by the green square in the figure is the result obtained by the equivalent LC circuit model. It can be found that the theoretical result is in good agreement with the numerical simulation results, further illustrating the validity of the equivalent LC circuit model in explaining the absorption characteristics of the system.

III. THE ABSORPTION PERFORMANCE OF CIRCULAR CAVITY AND ITS THEORETICAL EXPLANATION

Fig. 4(a) illustrates a one-dimensional metallic grating structure composed of a series of circular resonant cavities covered by the monolayer graphene. The diameter of the cavity is $w_3 = 2.1 \mu\text{m}$. A series of slits cut on the resonant cavity can couple the incident electromagnetic waves to the cavity. The width and the height of the slits are $w_2 = 0.608 \mu\text{m}$ and $h_2 = 0.1 \mu\text{m}$ respectively. Like the narrow slits described above, the cavity is filled with a kind of dielectric with a permittivity of 2.4. In fact, this is a typical microwave resonant cavity, where only electromagnetic waves with a certain frequency and a certain polarization direction can be coupled to the cavity to generate resonance phenomenon. Therefore, an ideal absorption peak can be obtained. Fig. 4(c) shows the absorption spectrum of the system obtained by FEM. Also, we can use CMT to explain the absorption performance of this system, the intrinsic loss rate δ and external leakage rate γ_e are $1.91 \times 10^{11} \text{ rad/s}$ and $3.16 \times 10^{11} \text{ rad/s}$ respectively. Fig. 3(d) illustrates that the results from CMT are basically consistent with the result from FEM.

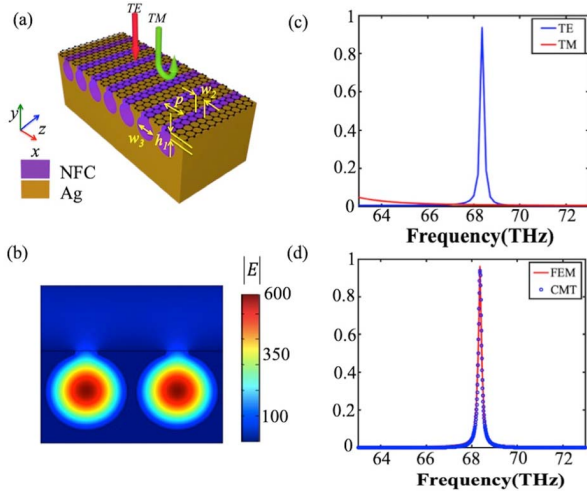


Fig. 4. (a) Schematic of the proposed one-dimensional structure. (b) The electric field ($|E|$) at the resonant frequency for TE polarization. (c) FEM simulated absorption spectrum of proposed structure for TE and TM polarization. (d) FEM simulated and CMT fitted absorption spectrum for TE polarization.

It can be found that under TE polarization, the system has formed a very narrow absorption peak with an absorption rate exceeding 97% whose center frequency is the same as the narrow cavity mentioned above. For TM polarization, no obvious resonance phenomenon can be observed, this is opposite of the narrow slits. The electric field distribution at the center frequency shown in Fig. 4(b) illustrates that this structure can localize most of the electric field in the center of the cavity because of the excitation of CMR, the calculation of resonance frequency of CMR can be obtained by the waveguide theory [22], [23]

$$f_{CMR} = \frac{c\sqrt{2(m/w_3)^2}}{2\eta\sqrt{\epsilon_d}} \quad (m = 1, 2, 3, \dots), \quad (13)$$

where $\eta = 0.954$ is the correction factor, m is a non-negative integer, and c is the speed of light in vacuum. The resonant frequency calculated by Eq. (10) is 68.35THz, which is basically consistent with the results from FEM.

In order to further verify the validity of Eq. (13), we have studied the influence of the geometric parameters of the resonators on the absorption performance of the system. As shown in Fig. 5(a), we investigated the influence of the diameter of the cavity on the resonance frequency under TE polarization. It was found that with the increase of the cavity diameter (from 1.5 μm to 2.2 μm), the resonance frequency of the system will show a significant red shift (reducing from 90 THz to 65.2 THz), and its absorption rate is always above 95%. In order to obtain higher-order cavity modes, we have adjusted the structure of the cavity slightly, and decomposed it into a combination of a circular cavity and a rectangular cavity with a height of h_3 . In this case, equation (13) needs to be adjusted to [24], [25]

$$f_{CMR} = \frac{c\sqrt{2(m/w_3)^2 + (n/h_3)^2}}{2\eta\sqrt{\epsilon_d}} \quad (m, n = 1, 2, 3, \dots), \quad (14)$$

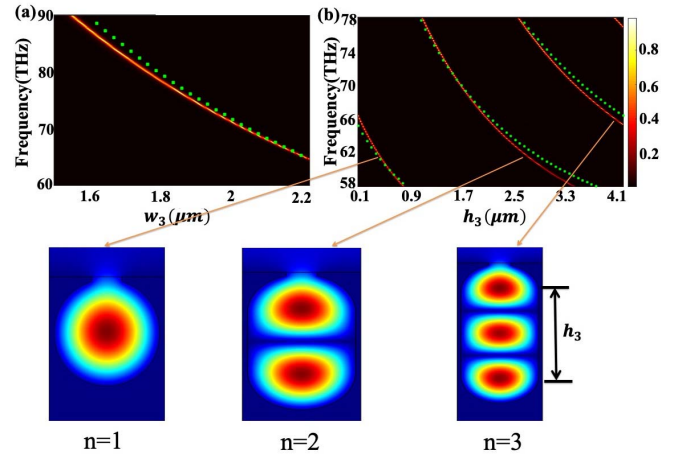


Fig. 5. Absorption spectrum as a function of (a) the frequency and cavity diameter w_3 and (b) the cavity depth h_3 .

We studied the influence of height h_3 on the absorption performance under TE polarization. From Fig. 5(b), it can be seen that as h_3 increases from 0 to 0.83 μm , the resonance frequency of the system also undergoes a significant redshift, which decreases from 68.32 THz to 58 THz. With h_3 increasing further, higher-order cavity modes appear. The curves indicated by the green square in Figs. 5 (a) and (b) are the results obtained by equations (13) and (14), which are basically consistent with the results obtained by FEM. These results indicate that the resonance frequency of the system can be completely predicted by the waveguide theory, and the occurrence of absorption peak is caused by the excitation of CMR under TE polarization.

IV. ABSORPTION PERFORMANCE OF COMPOUND METALLIC GRATING STRUCTURE

The above two types of resonate cavity are combined together to achieve the compound grating structure as shown in Fig. 6(a), which can form a broadband absorption peak under TM polarization and a narrow-band absorption peak under TE polarization, and the absorption frequencies of these two absorption peaks are the same. In order to test the stability of the device, we investigated the influence of the incidence angle on the absorption spectrum under different polarizations. The absorption as a function of incident frequency and incident angle are shown in Fig. 7(a) and Fig. 7(b). For the case of TM polarization, the resonance frequency and FWHM of the absorption spectrum changed little until the incident angle reaches to 35°. Therefore, the MR excited by the system is hardly affected by the incident angle within this range, as the incident angle continues to increase, the resonant frequency and maximum absorption of the system will change significantly due to the first-order diffraction effect of the grating. Also, for the TE polarization, the resonant frequency and FWHM of the system hardly change, and the maximum absorption rate remains above 95%. We attribute the incident angle insensitivity to the high symmetry of the two types of resonator structures thus the device is robust under oblique incidence [26]–[28]. The feature of angle insensitivity makes this device has high stability. In Fig. 7(c), we studied the

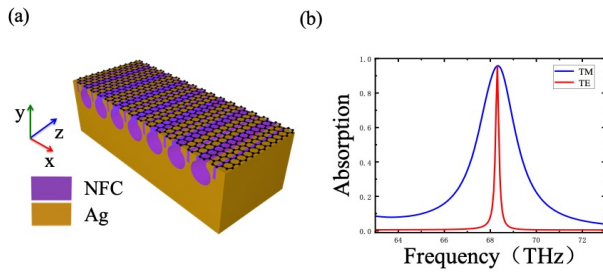


Fig. 6. (a) Schematic of the proposed one-dimensional absorber based on compound metallic grating. (b) FEM simulated absorption spectrum of proposed structure for TM and TE polarization.

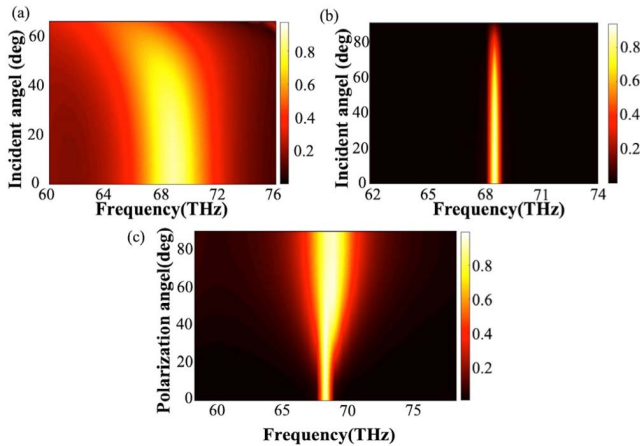


Fig. 7. The absorption spectrum as a function of incident angle for the (a) TM and (b) TE polarization. (c) The absorption spectrum for different polarization angles ranging from 0° (TE polarization) to 90° (TM polarization).

influence of the polarization angle of the incident electromagnetic wave on the absorption spectrum at normal incidence. We can find that as the polarization angle increases from 0° (TE polarization) to 90° (TM polarization) gradually, the resonance frequency always remains the same, and the absorptivity still remains very high (>95%), but the bandwidth will undergo a gradually increasing process. Therefore, this structure can have high sensitivity to the noticeable difference in bandwidth between absorption spectrums. Moreover, according to the electromagnetic field distribution in the two previous cases, we can achieve the transfer of the electromagnetic field in the two cavities by adjusting the polarization state of the incident polarized light.

V. THE OPTOMECHANICAL APPLICATIONS

Based on the above discussion of the absorption characteristics of the compound metallic grating structure, we can use it as a high-performance TE/TM mode switch. Firstly, it can be used as an absorber due to the broadband absorption spectrum under TM polarization. The narrowband absorption spectrum formed under TE polarization can also make the structure a great sensor. In order to test the performance of the sensor, we investigated how the reflective index (n_d) of the filled dielectric affect the absorption performance. As shown in Fig. 8(a), we can find that the resonant frequency will experience a red-shift as the reflective index increases, and as n_d increases further, the

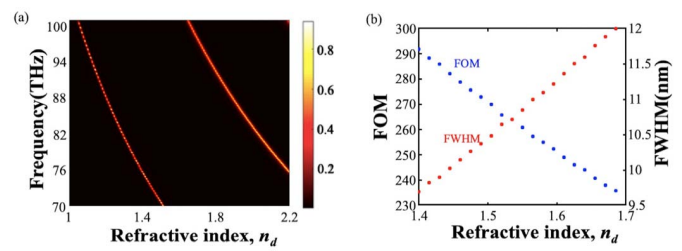


Fig. 8. (a) The absorption spectrum as a function of reflective index of the filled dielectric n_d under TE polarization. (b) The values of figure of merit (FOM) and FWHM for the first order mode with n_d ranging from 1.4 to 1.7.

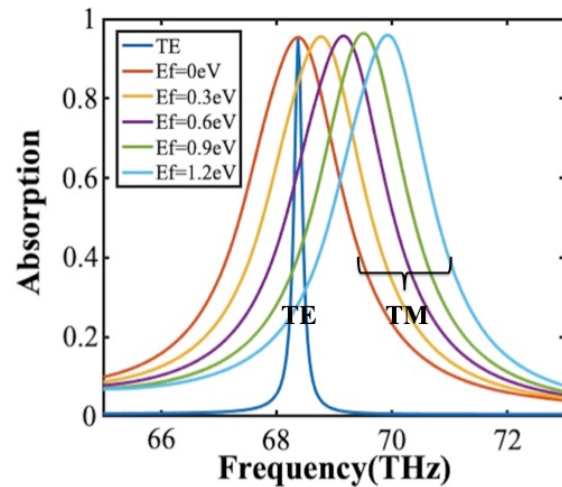


Fig. 9. Absorption spectrums of designed structure for different Fermi energy under TM and TE polarization.

second-order mode appeals. Then we calculated the sensitivity of the first-order mode S by using the equation (13), and the result shows that the value is 2829.46 nm/RIU, which is much higher than most of other sensors. In order to further evaluate the sensing performance of the structure, we studied the figure of merit (FOM) which can be expressed by $FOM = S/FWHM$. As shown in Fig. 8(b) despite the FOM undergoes a slight decrease while the reflective index increases from 1.4 to 1.7. Its value still remains very high (above 230), which outperforms most of other sensors. Generally speaking, sensors based on such circular resonant cavity can have very high sensitivity and FOM, and thus can play a superior performance in the reflective index sensing.

In addition, we can make full use of the special electromagnetic properties of graphene to adjust the absorption spectrum of this device. Fig. 9 shows the influence of the change of the Fermi energy on the absorption spectrum. We found that with the increase of Fermi energy, the broad absorption spectrum under TM polarization undergoes a blue-shift, nevertheless the narrow absorption spectrum under TE polarization will not be affected in any way. It is worth mentioning that the change of the fermi level does not cause the resonant modes of the structure to change. However, the increasing of the geometric parameters of cavity and refractive index of filled dielectric will lead to the occurrence of higher-order resonant modes as seen in Fig. 5(b) and Fig. 8(a). Therefore, the TE/TM mode

switch we designed based on the compound metallic grating is able to adjust functions as absorber or sensor easily by changing the polarization state of incident radiation. We can also make the absorption peak undergo a side shift by adjusting the Fermi energy of graphene to realize the regulation of absorption spectrum.

Moreover, the compound grating structure we design also has other potential applications in many aspects. For example, it can be used in optical fiber to design high sensing performance plasmonic sensors which will be very beneficial for bio- and gas-sensing applications [29]–[35]. In addition, the unique light absorption characteristics of such structure also make it an important application in spectral filtering [36]–[38].

VI. CONCLUSION

In conclusion, we have proposed a graphene-based metal-dielectric compound grating structure which can achieve high absorptivity under TE and TM polarization by optimizing its structural parameters. The absorption mechanisms are derived from the excitation of CMR and MR, which are well explained by waveguide theory and equivalent LC circuit mode. We have investigated the absorption spectrum of these two types of resonators separately and found that they have absorption spectrum with different line shapes when different polarized light is incident. According to this feature, we can use it to achieve a high-performance sensitive TE / TM mode switch functioning as absorber or sensor by adjusting the polarization states of incident radiations. More importantly, the absorber we designed is a kind of simple one-dimensional grating structure, which may greatly reduce the difficulty of manufacture.

REFERENCES

- [1] C.-H. Park, Y.-T. Yoon, and S.-S. Lee, "Polarization-independent visible wavelength filter incorporating a symmetric metal-dielectric resonant structure," *Opt. Express*, vol. 20, no. 21, p. 23769, 2012.
- [2] M. Diem, T. Koschny, and C. M. Soukoulis, "Wide-angle perfect absorber/thermal emitter in the terahertz regime," *Phys. Rev. B, Condens. Matter*, vol. 79, no. 3, Jan. 2009, Art. no. 033101.
- [3] Y. K. Srivastava, L. Cong, and R. Singh, "Dual-surface flexible THz fano metasensor," *Appl. Phys. Lett.*, vol. 111, no. 20, Nov. 2017, Art. no. 201101.
- [4] Y. Li, L. Yue, Y. Luo, W. Liu, and M. Li, "Light harvesting of silicon nanostructure for solar cells application," *Opt. Express*, vol. 24, no. 14, p. A1075, 2016.
- [5] H. S. Kim, S. H. Cha, B. Roy, S. Kim, and Y. H. Ahn, "Humidity sensing using THz metamaterial with silk protein fibroin," *Opt. Express*, vol. 26, no. 26, p. 33575, 2018.
- [6] T. Wang, M. Cao, H. Zhang, and Y. Zhang, "Tunable terahertz metamaterial absorber based on dirac semimetal films," *Appl. Opt.*, vol. 57, no. 32, p. 9555, 2018.
- [7] Y. Lu, J. Li, S. Zhang, J. Sun, and J. Q. Yao, "Polarization-insensitive broadband terahertz metamaterial absorber based on hybrid structures," *Appl. Opt.*, vol. 57, no. 21, p. 6269, 2018.
- [8] N. I. Landy, S. Sajuyigbe, J. J. Mock, D. R. Smith, and W. J. Padilla, "Perfect metamaterial absorber," *Phys. Rev. Lett.*, vol. 100, May 2008, Art. no. 207402.
- [9] J. Hao, L. Zhou, and M. Qiu, "Nearly total absorption of light and heat generation by plasmonic metamaterials," *Phys. Rev. B, Condens. Matter*, vol. 83, no. 16, Apr. 2011, Art. no. 165107.
- [10] M. Q. Ye, F. M. Hui, and J. C. Tie, "Strong coupling between magnetic plasmons and surface plasmons in a black phosphorus-spacer-metallic grating hybrid system," *Opt. Lett.*, vol. 13, no. 20, 2018, Art. no. 004985.
- [11] X. Zou, G. G. Zheng, J. W. Cong, L. H. Xu, Y. Y. Chen, and M. Lai, "Polarization-insensitive and wide-incident-angle optical absorber with periodically patterned graphene-dielectric arrays," *Opt. Lett.*, vol. 43, no. 1, 2018, Art. no. 000046.
- [12] S. Liu, H. B. Chen, and T. J. Cui, "A broadband terahertz absorber using multi-layer stacked bars," *Appl. Phys. Lett.*, vol. 106, no. 15, 2015, Art. no. 4918289.
- [13] Z. M. Zhang, "Nano/microscale heat transfer," *Int. J. Thermophys.*, vol. 29, no. 2, pp. 787–789, 2008.
- [14] G. W. Hanson, "Quasi-transverse electromagnetic modes supported by a graphene parallel-plate waveguide," *J. Appl. Phys.*, vol. 104, no. 8, pp. 705–709, 2008.
- [15] H.-J. Li, L.-L. Wang, B. Sun, Z.-R. Huang, and X. Zhai, "Controlling mid-infrared surface plasmon polaritons in the parallel graphene pair," *Appl. Phys. Express*, vol. 7, no. 12, Dec. 2014, Art. no. 125101.
- [16] Q. Lin, X. Zhai, L. Wang, B. Wang, G. Liu, and S. Xia, "Combined theoretical analysis for plasmon-induced transparency in integrated graphene waveguides with direct and indirect couplings," *EPL (Europhys. Lett.)*, vol. 111, no. 3, p. 34004, Aug. 2015.
- [17] A. Li and W. Bogaerts, "Tunable electromagnetically induced transparency in integrated silicon photonics circuit," *Opt. Express*, vol. 25, no. 25, p. 31688, 2017.
- [18] J. R. Piper and S. H. Fan, "Total absorption in a graphene monolayer in the optical regime by critical coupling with a photonic crystal guided resonance," *ACS Photon.*, vol. 1, no. 4, p. 1021, 2014.
- [19] Z. Ruan and S. Fan, "Temporal coupled-mode theory for light scattering by an arbitrarily shaped object supporting a single resonance," *Phys. Rev. A, Gen. Phys.*, vol. 85, no. 4, Apr. 2012, Art. no. 043828.
- [20] B. Zhao and Z. M. Zhang, "Study of magnetic polaritons in deep gratings for thermal emission control," *J. Quant. Spectrosc. Radiat. Transf.*, vol. 81, no. 89, p. 135, 2014.
- [21] L. P. Wang and Z. M. Zhang, "Phonon-mediated magnetic polaritons in the infrared region," *Opt. Express*, vol. 2, no. 6, p. 1364, 2011.
- [22] R. Feng, J. Qiu, Y. Cao, L. Liu, W. Ding, and L. Chen, "Omnidirectional and polarization insensitive nearly perfect absorber in one dimensional meta-structure," *Appl. Phys. Lett.*, vol. 105, no. 18, Nov. 2014, Art. no. 181102.
- [23] H. Sai and H. Yugami, "Thermophotovoltaic generation with selective radiators based on tungsten surface gratings," *Appl. Phys. Lett.*, vol. 85, no. 16, pp. 3399–3401, Oct. 2004.
- [24] S. Maruyama, T. Kashiwa, H. Yugami, and M. Esashi, "Thermal radiation from two-dimensionally confined modes in microcavities," *Appl. Phys. Lett.*, vol. 79, no. 9, pp. 1393–1395, 2001.
- [25] F. Kusunoki, T. Kohama, T. Hiroshima, S. Fukumoto, J. Takahara, and T. Kobayashi, "Narrow-band thermal radiation with low directivity by resonant modes inside tungsten microcavities," *Jpn. J. Appl. Phys.*, vol. 43, no. 8A, pp. 5253–5258, Aug. 2004.
- [26] Y. T. Zhao, B. Wu, B. J. Huang, and Q. Cheng, "Switchable broadband terahertz absorber/reflector enabled by hybrid graphene-gold metasurface," *Opt. Express*, vol. 25, no. 7, p. 7161, 2017.
- [27] C. H. Lin, R. L. Chern, and H. Y. Lin, "Polarization-independent broadband nearly perfect absorbers in the visible regime," *Opt. Express*, vol. 19, no. 2, pp. 415–424, 2011.
- [28] J. M. J. Ma, D. L. D. Liu, J. W. J. Wang, and Z. H. Z. Hu, "Plasmonic sensor with variable claddings based on metallic slit arrays," *Chin. Opt. Lett.*, vol. 16, no. 3, 2018, Art. no. 032301.
- [29] Z. Bao *et al.*, "Coordinated multi-band angle insensitive selection absorber based on graphene metamaterials," *Opt. Express*, vol. 27, no. 22, pp. 31435–31445, 2019.
- [30] W. He *et al.*, "Sensors with multifold nanorod metasurfaces array based on hyperbolic metamaterials," *IEEE Sensors J.*, vol. 20, no. 4, pp. 1801–1806, Feb. 2020.
- [31] Á. González-Vila, A. Ioannou, M. Loyez, M. Debliquy, D. Lahem, and C. Caucheteur, "Surface plasmon resonance sensing in gaseous media with optical fiber gratings," *Opt. Lett.*, vol. 43, no. 10, pp. 2011–2308, 2018.
- [32] A. K. Sharma and C. Marques, "Design and performance perspectives on fiber optic sensors with plasmonic nanostructures and gratings: A review," *IEEE Sensors J.*, vol. 19, no. 17, pp. 7168–7178, Sep. 2019.
- [33] C. Caucheteur, T. Guo, F. Liu, B.-O. Guan, and J. Albert, "Ultrasensitive plasmonic sensing in air using optical fibre spectral combs," *Nature Commun.*, vol. 7, no. 1, p. 13371, Dec. 2016.
- [34] A. K. Sharma, B. Kaur, and C. Marques, "Simulation and analysis of 2D material/metal carbide based fiber optic SPR probe for ultrasensitive cortisol detection," *Optik*, vol. 218, Sep. 2020, Art. no. 164891.
- [35] A. K. Pandey, A. K. Sharma, and C. Marques, "On the application of SiO₂/SiC grating on ag for high-performance fiber optic plasmonic sensing of cortisol concentration," *Materials*, vol. 13, no. 7, p. 1623, Apr. 2020.

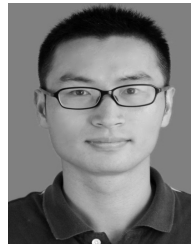
- [36] A. K. Pandey, A. K. Sharma, and C. Marques, "On the application of stacked periodic tungsten grating nanostructure in wide-range plasmonic sensing and other photonic devices," *Plasmonics*, pp. 1–9, Aug. 2020.
- [37] J. Wang, L. Yang, Z.-D. Hu, W. He, and G. Zheng, "Analysis of graphene-based multilayer comb-like absorption system based on multiple waveguide theory," *IEEE Photon. Technol. Lett.*, vol. 31, no. 7, pp. 561–564, Apr. 1, 2019.
- [38] J. Wang *et al.*, "Perfect absorption and strong magnetic polaritons coupling of graphene-based silicon carbide grating cavity structures," *J. Phys. D, Appl. Phys.*, vol. 52, no. 1, 2019, Art. no. 015101.



Tairong Bai was born in Sichuan, China, in 1999. He is currently a Junior Undergraduate with the Department of Photoelectric Information Science and Engineering, School of Science, Jiangnan University. His research interests include micro-nano optical devices and metamaterials. He is a member of the Prof. Jicheng Wang's Research Team.



Yang Tang was born in Henan, China, in 1998. Since 2017, she has been a Junior with the School of Science, Jiangnan University. She is mainly engaged in perfect absorption. Her research interests include perfect absorption of graphene-based silicon carbide grating structures and metamaterials. She is a member of the Prof. Jicheng Wang's Research Team.

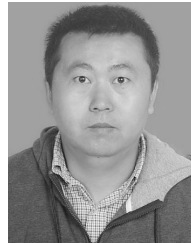


Zheng-Da Hu received the Ph.D. degree in physics from Zhejiang University in 2013. He is currently an Associate Professor with the Department of Photoelectric Information Science and Engineering, School of Science, Jiangnan University. His research interests include quantum optics, quantum information, and quantum plasmonics.

Tonglu Xing, photograph and biography not available at the time of publication.

Zhiyu Lu, photograph and biography not available at the time of publication.

Yulan Huang, photograph and biography not available at the time of publication.



Jicheng Wang received the Ph.D. degree in optics from the Harbin Institute of Technology, Harbin, Heilongjiang, China, in 2011. He worked as a Postdoctoral Researcher with the School of Mechanical Engineering, Purdue University, West Lafayette, IN, USA. He is an Associate Professor with the School of Science, Jiangnan University, Wuxi, Jiangsu, China. His research interests include plasmonics, nano photonics, metasurface and metamaterials, quantum plasmonics, and informations.